5804 *Macromolecules* **2010**, *43*, 5804–5813
DOI: 10.1021/ma100841c

Macromolecules
ARTICLE

Micrometer and Submicrometer Particles Prepared by Precipitation Polymerization: Thermodynamic Model and Experimental Evidence of the Relation between Flory's Parameter and Particle Size

Antonio L. Medina-Castillo,* Jorge F. Fernandez-Sanchez,* Antonio Segura-Carretero, and Alberto Fernandez-Gutierrez

Department of Analytical Chemistry, University of Granada, Avd. Fuentenueva s/n, 18071 Granada, Spain

Received April 16, 2010; Revised Manuscript Received May 31, 2010

ABSTRACT: This work highlights the relevance of the interactions between polymer and solvent during precipitation polymerization in order to control the morphology and the size of the precipitated material without any changes in chemical composition. Thus, a thermodynamic model based on Flory Hugings model and Hansen's solubility parameters has been proposed in order to control the precipitation process. This model is based on the study and characterization of the interactions (hydrogen-bonding forces, polar forces and dispersion forces) between growing polymeric chains and solvent molecules. The model was corroborated by more than 80 different solvent compositions were used for a ternary solvent mixture (toluene, acetonitrile and 2-propanol) and two different monomer molar ratio feeds (45% MAA, 20% HEMA, and 35% EDMA; 20% MAA, 45% HEMA, and 35% EDMA). The morphologies of the resulting polymer material were characterized by scanning electron microscopy and transmission electron microscopy and the particles sizes were deduced by dynamic light scattering. The polymeric particles with different sizes prepared in this work were used to introduce on them magnetic properties. The results in this work enable the control of the size, chemical composition, and the homogeneous encapsulation of Fe_3O_4 within different hydrophilic polymeric matrixes by polymerization precipitation, allowing the design of magnetic particles free of any stabilizers.

1. Introduction

Copolymer microspheres are attractive for many applications, due to their unique morphology and designed surface properties. For instance, uses as adsorbents, stationary phases for chromatography, supports for exchange, membrane materials, catalysis, sensors, and carriers as well as supports in biomedical and environmental fields, are possible due to their unique morphology and designed surface properties.[1−5] Therefore, the control of the surface properties of particles is key in many areas and in numerous commercial technologies, ranging from biotechnology to advanced microelectronics.[6,7]

Emulsion, suspension, and dispersion polymerization are well-known techniques for preparing copolymer microspheres and nanospheres. However, it is often tedious to remove the surfactant or stabilizer necessary for stabilizing of the microspheres during their preparation.

Precipitation polymerization is unique to prepare polymeric microspheres of uniform size and shape free of any added surfactant or stabilizer. This technique starts as a homogeneous mixture of monomer, initiator, and optional solvents, and during the polymerization, the growing polymeric chains are separated from the continuous medium by changes in the mixing free energy.[8]

In recent years, precipitation polymerization has been widely used to prepare narrow or monodispersed microspheres with different functional chemical groups on their surfaces, in the absence of any stabilizer or additive, and without stirring. The control of the size and the uniformity of the resulting polymeric particles has been major area of interest, especially for particles in the micrometer and submicrometer size range.

A main disadvantage is the difficulty in obtaining monodispersed hydrophilic polymeric microspheres with good spherical shape by this polymerization technique.[9] Several experiments have been carried out to establish the effect of the initial molar monomers (which contain hydroxyl and acid groups such as MAA and HEMA) ratio feed on the morphology and size of microspheres produced by precipitation polymerization in nonpolar solvents.[10−12] Less attention has been paid to the effects of the microspheres on the morphology and size by the changes caused in the interactions between polymeric growing chains and solvent molecules when the initial molar monomers ratio feed is kept constant.In addition, the previously reported data are rather qualitative since they may require tedious theoretical thermodynamic treatments.

This paper describes a thermodynamic model based on the Flory−Huggins model and Hansen solubility parameters, allowing us to delve into knowledge of the precipitation process in precipitation polymerization. This model is based on the study and characterization of the interactions (hydrogen bonding and polar and dispersion forces) between growing polymeric chains and solvent molecules, because change in these interactions provides the desolvation and collapse of the network at different growth levels. This phenomenon is analogous to the cloud point observed when a solution containing one homopolymer is heated above the lower critical solution temperature (LCST).[10]

Correlations between the morphology of the polymeric network (soluble copolymer, macrogels, gels, and spherical colloids) with the polymer−solvent interactions will be given in order to

*Corresponding authors. (A.L.M.C.) Telephone: +34 958248593. Fax: +34 958249510. E-mail: antonioluismedina@ugr.es. (J.F.F.-S.) Telephone: +34 958248409. Fax: +34 958249510. E-mail: jffernan@ugr.es.

 Published on Web 06/10/2010

show the versatility of the model. In addition, this model can be used to correlate the particle size of spherical colloids with the polymer−solvent interactions. Therefore, the model allows micrometer and submicrometer particles of different sizes to be synthesized without changing the molar monomer ratio feed.

Finally, hydrophilic magnetic micrometer and submicrometer particles were synthesized by precipitation polymerization.

2. Theory

2a. Flory−Huggins Model and Hansen Solubility Parameters. According to the Flory−Huggins theory for polymer solutions, the free energy of a mixture is:[13−15]

$$\Delta G_{mix} = n_s RT\chi_{s,p}\Phi_p + RT[n_s \ln \Phi_s + n_p \ln \Phi_p] \quad (1)$$

where enthalpic and entropic contributions are given by:

$$\Delta H_{mix} = n_s RT\chi_{s,p}\Phi_p, \quad \Delta S_{mix} = RT[n_s \ln \Phi_s + n_p \ln \Phi_p] \quad (2)$$

The subscripts s and p are the corresponding labels for solvent and polymer, respectively, $\chi_{p,s}$ is the Flory's parameter which is related with the interaction between solvent molecules and polymer segments, Φ is the volume fraction, and the parameter x is often interpreted as the number of lattice segments occupied by a given polymer and it is estimated as the volume molar ratio of polymer and solvent.[13−16] The volume fraction of the polymer can be expressed as

$$\Phi_p = \frac{xN_p}{N_0} \quad (3)$$

where N_p is the number of polymer molecules and N_0 is the total numbers of molecules (solvent and polymer). For diluted polymer solutions, small changes in the polymer molecular weight (x) do not result in large increases of Φ_p (see eq 3).

In addition, the Flory parameter $\chi_{s,p}$ is related to the coordination number of the lattice (z) and the interchange energy (Δw) by the following expression:[17]

$$\chi_{s,p} = -\frac{z\Delta w}{2RT} \quad (4)$$

Here the interchange energy, Δw, is the energy difference involved in breaking a solvent−solvent interaction (w_{ss}) and a polymer-segment−polymer-segment interaction (w_{pp}) to form two solvent−polymer-segment interactions (w_{sp}):

$$\Delta w = (w_{ss} + w_{pp}) - 2w_{sp} \quad (5)$$

Also, Δw can be interpreted as an free-energy exchange with enthalpic and entropic contributions:[17]

$$\Delta w_G = \Delta w_H - T\Delta w_S \quad (6)$$

and thus,

$$\chi_{s,p} = \chi_{s,p,H} + \chi_{s,p,S} = -\frac{z\Delta w_H}{2RT} + \frac{z\Delta w_S}{2R} \quad (7)$$

In addition, $\chi_{s,p}$ is related with the polymer size, i.e., with the average molecular weight of a polymer; an increase in the average molecular weight provides an increase of the $\chi_{s,p}$. This has been experimentally demonstrated,[17,18] but there is not any theoretical relation between molecular weight and Flory's parameter.

On the other hand, it is possible to correlate the Flory's parameter with Hansen's solubility parameters. Hansen divided the solubility parameters into contributions for dispersion (δ_d), dipole (δ_p), and hydrogen-bonding (δ_h) interactions.[19] It is possible to express the solubility parameters for a mixture of i solvents as

$$\overline{\delta}_{i,j} = \sum_i \phi_i \delta_{i,j}; \quad j = d, p, h \quad (8)$$

where $\overline{\delta}_j$ is the j solubility parameter of the mixture, Φ_i is the volume fraction of solvent i and $\delta_{i,j}$ is the solubility parameter j of solvent i.[20] This expression may be applied for an ideal mixture of solvents with similar molar volumes.

The solubility parameter model has been successful in describing thermodynamic properties of polymer solutions. It shows that the Flory's parameter can be related to the three-dimensional solubility parameters[21,22] by

$$\chi_{s,p} = \left(\frac{V_s}{RT}\right) {R_{s,p}}^2 \quad (9)$$

where V_s is the molar volume of the solvent when using one solvent or an average molar volume in solvent mixtures,[18,22] and ${R_{s,p}}^2$ is a modified difference between the Hansen solubility parameter for a solvent (s) and a polymer (p).

A useful concept that quantifies the similarity of polymer, p, and solvent, s, is the solubility parameter distance ($R_{s,p}$),[22] defined by

$$R_{s,p} = [4(\delta_{d,p} - \delta_{d,s})^2 + (\delta_{p,p} - \delta_{p,s})^2 + (\delta_{h,p} - \delta_{h,s})^2]^{1/2} \quad (10)$$

This means that the polymer solvent interactions increase when the solubility parameter distances decrease. When $\chi_{s,p}$ is less than 0.5, the solvent is generally classified as a good solvent for the polymer, while a value higher than 0.5 is a poor solvent and may lead to phase separation.[23] It can be applied in mixtures of the two and three noninteracting solvent systems.[9,18,22−26]

The three-dimensional Hansen's solubility parameters can be simplified into a dimensional one.[27] Therefore, three-dimensional coordinates (δ_p, δ_d and δ_h) are converted into two-dimensional coordinates ($PD_{s,p}$ and $H_{s,p}$). The relation between $PD_{s,p}$ and $H_{s,p}$ parameters with δ_p, δ_d and δ_h is

$${PD_{s,p}}^2 = 4(\delta_{d,s} - \delta_{d,p})^2 + (\delta_{p,s} - \delta_{p,p})^2 \quad (11)$$

$${H_{s,p}}^2 = (\delta_{h,s} - \delta_{h,p})^2 \quad (12)$$

where the subscripts s and p denote the solvent mixture and polymer, respectively. Thus, $PD_{s,p}$ can be used to characterize dispersion and polar interactions between the polymeric growing chains and solvent, and $H_{s,p}$ the hydrogen bonding interactions between the polymeric growing chains and solvent.

With eqs 10, 11, and 12, the solubility parameter distance ($R_{s,p}$) can be rewritten as

$$R_{s,p} = ({PD_{s,p}}^2 + {H_{s,p}}^2)^{1/2} \quad (13)$$

2b. Precipitation Mechanism. It is well-known that the particle formation by polymerization precipitation consists with two stages: nucleation and growth.[28] Therefore, the

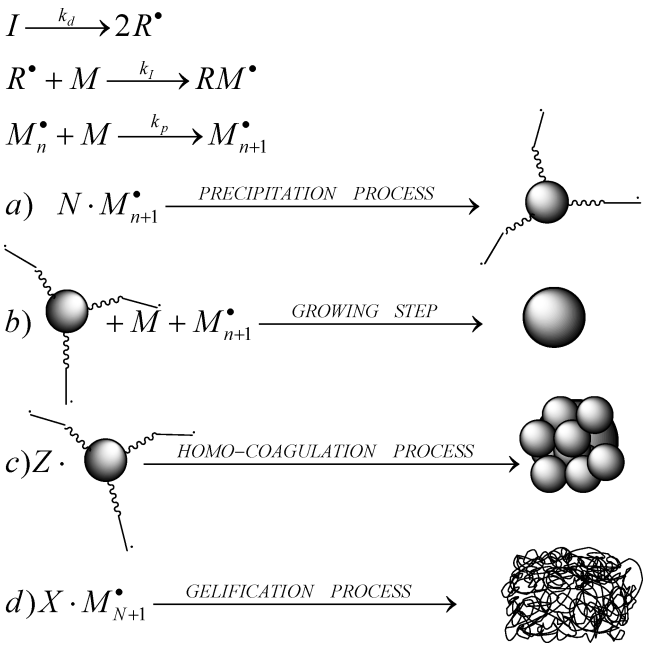

Figure 1. Different steps for the formation of different polymeric network morphologies by precipitation polymerization. Key: radical initiator (I), monomer (M), and polymeric growing chains (M_{N+1}, M_{n+1}; N and n indicate the average number of monomers forming the polymeric chain, $N > n$).

system is homogeneous prior precipitation and, as soon as the polymerization starts, primary radicals, generated by decomposition of the initiator, grow by the addition of monomer units and provide solvated polymeric growing chains (monophasic system). This occurs until the systems reach to their maximum molecular weight, which can be solvated by the media. At this moment, when the media cannot solvate the polymeric growing chains, the separate-phase and precipitation process starts, and N polymeric growing chains interact spontaneously with each other to produce the precipitation[28] (see Figure 1, step a) thus the transparent and homogeneous reaction mixture becomes a milky white dispersion. Finally, the particle growing step can happen in two ways:[29] 1) by capturing oligomer radical and monomer on the particle surface (see Figure 1, step b), or 2) by aggregation of nuclei to form the mature particles by a homocoagulation process (see Figure 1, step c). If the solvent medium is suitable, the polymeric chains grow too much and they precipitate as a gel (see Figure 1, step d).

3. Experimental Section

3a. Experimental Conditions Used for Precipitation Polymerization. In this work, all the experiments were performed without stirring, maintaining constant molar monomers and cross-linked ratio feed, using diluted concentrations of monomers (2.5% w/v), a pressure of 1 atm, a temperature of 82 °C, a reaction time of 1.30 h, and a total volume of solvent media of 16 mL. The conditions for selecting solvents, monomers, and radical initiator were as follows:

(a) The solvents should be selected to provide an ideal mixture, or at least as ideal as possible.[24,32]
(b) The monomers should be compatible; hence the reactivity ratio between the monomers and cross-linker is related to the formation of a statistical polymer during the polymerization reaction.
(c) Monomers and solvents must be miscible with respect to each other, and the radical initiator must be soluble in this monomer−solvent mixture.

With these conditions, the solvents selected were: toluene, acetonitrile, and 2-propanol; the monomers were hydroxyethyl methacrylate (HEMA) and methacrylic acid (MAA); the cross-linker was ethylenglycol dimethacrylate (EDMA); and the radical initiator was azobis(isobutyronitrile) (AIBN). In this work, two different molar monomer ratio feeds were used (45% MAA−20%HEMA−35%EDMA, called P1, and 20%MAA−45%HEMA−35%EDMA, called P2).

3b. Magnetic Hybrid Nanoparticles Encapsulated by EDMA/MMA/HEMA (EDMA/MMA/HEMA−Fe_3O_4−OA). Magnetite coated with oleic acid (lipophilic magnetic nanoparticles) was prepared by the conventional method.[31] Then, 2 g of lipophilic magnetic nanoparticles were dispersed in 5 mL of *n*-heptane and added to 400 mL of Milli-Q water containing 250 mg of SDS. The ice-cooled mixture was sonicated for 20 min in a high-energy sonifier (BRANSON, S-450D) at 70% amplitude for 20 min. The resulting mini-emulsion was transferred slowly (under mechanical stirring) to a double-necked flask containing 1.5 mL of 26 wt % MMA, 60 wt % EDMA, and 14 wt % HEMA. The mixture was stirred for 2 h at room temperature. Next, 180 mg of potassium peroxodisulfate (KPS) was added to start the polymerization, and the reaction system was heated to 65 °C under a gentle stream of nitrogen. After a polymerization time of 24 h, the resulting product was washed six times with Milli-Q water, five times with acetone, and five times with methanol in order to eliminate surfactant and unreacted compounds.

3c. Magnetic Particles Containing EDMA/MMA/HEMA−Fe_3O_4−OA Prepared by Precipitation Polymerization. The experimental conditions to prepare magnetic particles by precipitation polymerization were selected taking into account the results found in the control of particle size for systems P1 and P2. Two different conditions were selected: (1) the experimental conditions to obtain 1100 nm particles of P1 and (2) the experimental conditions to obtain gels for P1 and P2 systems. Precipitation polymerizations were developed in the presence of 5 wt % (with respect to the monomer mixture) of the EDMA/MMA/HEMA-Fe_3O_4−OA nanoparticles prepared in section 3b following the protocol described in section 3a.

3d. Morphological Characterization. The particles prepared in this work were washed with methanol several times and then the particle size was measured in methanol by dynamic light scattering (Zetasizer Nano ZS-90, Malvern Instrument). The morphology of the materials prepared in this work was analyzed by scanning electron microscopy (SEM) and high resolution transmission electron microscopy (HRTEM).

4. Results and Discussion

4a. Assumptions To Model the Precipitation and Formation of Different Polymeric Network Morphologies. Under the experimental conditions mentioned above and making an appropriate selection of solvents (ideal mixture) and monomers for the formation of the statistical polymer (see section 3a), we propose the following assumptions:

(a) The polymeric chains grow solvated by the media ($\Delta G_{mix} < 0$) and the precipitation process starts at the propagation step.
(b) The chemical composition of the polymeric growing chains before precipitation does not change; they grow by repetitions of a minimum statistical polymer unit.
(c) The average molecular weight of the polymeric growing chains before precipitation depends on the Flory's parameter value. Lower values of Flory's parameter before precipitation provide greater growing of the solvated polymeric chains.
(d) The phase separation and precipitation for forming spherical particles occur rapidly and spontaneously.
(e) The area or size of the final particles for stable suspensions formed by spherical particles depends of the average molecular weight of the polymeric

growing chains just before precipitation. It means that higher average molecular weights before precipitation provide higher final particles size and vice versa.

4b. Qualitative Thermodynamic Analysis of the Precipitation and Formation of the Different Polymeric Network Morphologies. Assuming that the precipitation step for obtaining stable colloidal suspensions could be considered as a hypothetical chemical reaction, the solvated polymeric growing chains just before precipitation would be considered reactants, the particles that constitute the stable colloidal suspension just after separate phase would be the products, and ΔG_{prec} would be the free energy of the precipitation processes (see Figure 1, step a). Therefore, a qualitative thermodynamic analysis of the precipitation processes can be carried out by considering the Flory−Huggins model and the Hansen solubility parameters.

In general, solubility, or miscibility of solvent and polymer, is to be expected if there is a decrease in the free energy of mixing. Inasmuch as the entropy of mixing ΔS_{mix} is always positive (i.e., $-T\Delta S_{mix} < 0$) the enthalpy of mixing will virtually determine the solubility.[21]

Considering the precipitation process as the opposite of the mixing, we can consider $-T\Delta S_{prec} > 0$. Therefore, ΔS_{prec} and ΔH_{prec} must be negative and therefore we can conclude that precipitation occurs when

$$|\Delta H_{prec}| > T|\Delta S_{prec}| \tag{14}$$

Before precipitation, the polymeric growing chains are solvated (monophasic system); this means that ΔG_{prec} is positive and ΔG_{mix} is negative.[21] Then, these chains continue growing and their average molecular weight is increased. As commented before, an increase in the average molecular weight increases Flory's parameter and hence increases $R_{s,p}$ (see eq 9). The free energy of a mixing can be related with the Flory's parameter (see eq 1).[18,30] Thus, greater molecular weight results in an increase in the ΔH_{mix} and therefore of ΔG_{mix} (see eqs 1 and 2). Therefore, sometime during the polymerization reaction, the value of $\Delta G_{mix} = 0$. We define this moment as the inflection or critical point (I.C.).

At this point, under the experimental condition mentioned above, the Flory's parameter at the I.C. point ($\chi_{s,p,IC}$) can be calculated by eq 9. For this we have to consider assumption b (see section 3a), which allows the calculation of the minimum statistical polymer unit and therefore the value of its Hansen solubility parameter, and the Hansen solubility parameters of the solvent mixture at I.C. point.

With assumptions d and e (see section 4a), it is possible to establish a relationship between average molecular weight of the polymeric growing chains and particle size. Bearing in mind that average molecular weight can be related with the Flory's parameter, we can say that

$$\text{particle size} = f(\chi_{s,p,IC}) \tag{15}$$

We will demonstrate that for evaporation lower than 20% of the initial volume of solvent mixture, the composition of the solvent mixtures is practically constant before precipitation. Thus, Flory's parameter at the IC point ($\chi_{s,p,IC}$) can be approximated to the initial Flory's parameter ($\chi_{s,p,0}$), and eq 15 can be rewritten as follows:

$$\text{particle size} = f(\chi_{s,p,0}) \tag{16}$$

This consideration will be demonstrated experimentally in section 4c. In addition, we will demonstrate that it is possible to control the particle size in a wide range by changing the solvent media without changing the molar ratio of monomers and cross-linked feed.

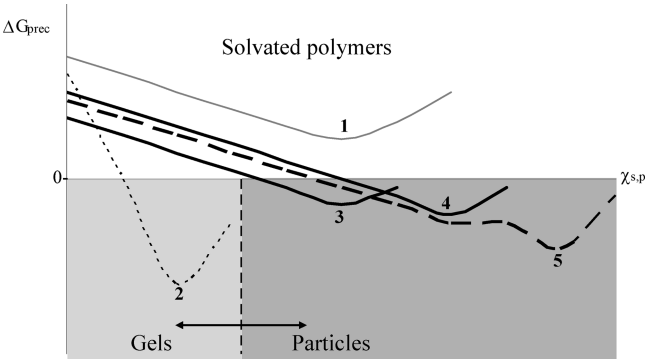

Figure 2. Qualitative thermodynamic diagrams to analyze the different polymeric network morphologies versus $\chi_{s,p}$ and the shape of the variation of ΔG_{prec} during the polymerization for the formation of a statistical copolymer in ideal mixtures of solvents. One (gray lines) corresponds with solvated copolymers; 2 (thin short-dash black line) correspond with a gel; 3 and 4 (bold black line) correspond with spherical particles of different size (the size of 3 is higher than the size of 4); 5 (bold dash line) corresponds with a nonspherical particle formed by homocoagulation process.

To continue with the polymerization process, after I.C. point, the phase separation and precipitation process starts. Separate-phase and precipitation process will continue until the ΔG_{prec} rises to a minimum value. The polymeric network morphologies can be related with the value of the Flory's parameter at the I.C. point, and the number of times that ΔG_{prec} reaches a minimum value after arriving at the I.C. point (see Figure 2).

A small value of Flory's parameter at the I.C. point means that the average molecular weight of the polymeric growing chains is high, so that, after the I.C. point they should precipitate by forming an amorphous material (gel). Otherwise, a high value of Flory's parameter at I.C. point means that the average molecular weight of the polymeric growing chains just before precipitation is short, so their precipitation provides particulate materials. This approach will be confirmed by experimental data in section 4e. Also, the ranges of Flory's parameter in which the different materials are obtained will be determined in section 4f.

The particulate material can be spherical particles or nonspherical particles formed by a homocoagulation process. This depends of the numbers of times that ΔG_{prec} reaches a minimum value after the I.C. point. If ΔG_{prec} reaches only a minimum value once, narrow disperse spherical particles result. If ΔG_{prec} reaches to a minimum value twice, spherical particles are produced first, and then coagulation processes between particles occur, giving rise to nonspherical particles formed by the homocoagulation process (see Figure 2).

4c. Relationship between Initial and I.C. Point Flory's Parameters. In this section, we will demonstrate that eq 15 can be rewritten as eq 16, and therefore $\chi_{s,p,IC} \approx \chi_{s,p,0}$.

If the composition of the solvent mixture changes by evaporation, Flory's parameter also changes during polymerization. To analyze the effect of solvent evaporation on the Flory's parameter, we evaluated four solvent compositions. The first is based on a unique solvent (acetonitrile), and thus the Flory's parameter is not affected by evaporation. The molar fraction of each solvent in the other three compositions were as follows: composition 2, $X_{\text{Toluene}} = 0.5$, $X_{\text{Acetonitrile}} = 0.25$, $X_{\text{2-Propanol}} = 0.25$; composition 3, $X_{\text{Toluene}} = 0.6$, $X_{\text{Acetonitrile}} = 0.25$, $X_{\text{2-Propanol}} = 0.15$; composition 4, $X_{\text{Toluene}} = 0.3$, $X_{\text{Acetonitrile}} = 0.35$, $X_{\text{2-propanol}} = 0.35$). The monomer feed molar percentage was 45% MAA, 20% HEMA and 35% EDMA (P1 system, see section 3a).

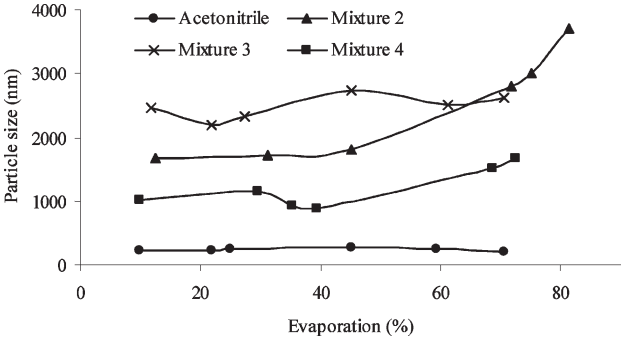

Figure 3. Effect of the solvent evaporation during polymerization over the final particle size. Mixture 2: $X_{\text{Toluene}} = 0.5$, $X_{\text{Acetonitrile}} = 0.25$, $X_{\text{2-Propanol}} = 0.25$. Mixture 3: $X_{\text{Toluene}} = 0.6$, $X_{\text{Acetonitrile}} = 0.25$, $X_{\text{2-Propanol}} = 0.15$. Mixture 4: $X_{\text{Toluene}} = 0.3$, $X_{\text{Acetonitrile}} = 0.35$, $X_{\text{2-Propanol}} = 0.35$.

To control the evaporation of solvents, we used different nitrogen flows (0, 10, 15, 20, 30, and 35 mL min^{-1}). The evaporated solvent was collected in a cool trap. Figure 3 shows the effect of solvent evaporation on particle size. We see that the evaporation does not affect the final particle size when pure acetonitrile is used as solvent. For mixtures 2, 3, and 4, the final particle sizes are not affected by solvent evaporations lower than 20%.

In this paper, we consider only the systems in which the total evaporation percentage is lower than 20% of the initial volume. Bearing this in mind and the fact that the cloud point is reached at 5 to 10 min, we can conclude by assumption b (see section 4a) that the Flory's parameter at I.C. (which is reached before cloud point) can be considered equal to the initial Flory's parameter.

4d. Estimation of the Hansen's Solubility Parameters of Solvents and Polymeric Growing Chains. To enable the relation between particle size and $\chi_{s,p,0}$, it is necessary to know its value; $\chi_{s,p,0}$ can be calculated by using $R_{s,p,0}$ (see eq 9), and $R_{s,p,0}$ can be calculated by using the Hansen's solubility parameter of the solvent mixture and the polymeric growing chains (see eq 10).

The Hansen solubility parameters of the polymeric growing chains can be calculated by using the second initial premise (see section 4a, premise b), which allows the characterization of the polymeric growing chains by the minimum statistical polymer unit and by using the incremental method proposed by Hoftycer and van Krevelen.[7,18,27] This method is based on group-attraction constants for dispersion (F_{di}) and polar (F_{pi}) components, and group cohesion energies (E_{hi}); some data are presented in Table 1. Thus, Hansen's solubility parameter for the each solvent and the minimum statistical polymer unit can be calculated by

$$\delta_h = \sqrt{\frac{\sum_{i=1}^{n} Eh_i}{\sum_{i=1}^{n} V_i}} \tag{17}$$

$$\delta_p = \frac{\sqrt{\sum_{i=1}^{n} F^2{}_{pi}}}{\sum_{i=1}^{n} V_i} \tag{18}$$

$$\delta_d = \frac{\sum_{i=1}^{n} Fd_i}{\sum_{i=1}^{n} V_i} \tag{19}$$

Table 1. Group Increments for Calculating the Solubility Parameters of Statistical Polymeric Minimum Units in P1 and P2 Systems[18]

	E_{hi} (J mol^{-1})	F_{pi} ($J^{1/2}$ $cm^{3/2}$ mol^{-1})	F_{di} ($J^{1/2}$ $cm^{3/2}$ mol^{-1})	V_i (cm^3 mol^{-1})
−COOH	10 000	420	530	28.5
−OH	20 000	500	210	10
−COO−	7000	490	390	18
$-CH_3$	0	0	420	33.5
$-CH_2-$	0	0	270	16.1
>CH−	0	0	80	−0.1
>C<	0	0	−70	−19.2

Table 2. Estimation of the Hansen Solubility Parameter of Solvents and Polymeric Growing Chains of P1 and P2

	δ_p ($MPa^{1/2}$)	δ_d ($MPa^{1/2}$)	δ_h ($MPa^{1/2}$)
P1	0.74	17.2	11.5
P2	1.2	18.9	12.2
toluene	1.54	18.8	0
acetonitrile	19.1	14.8	6.6
2-propanol	6.6	14.9	16.2

Table 2 shows the Hansen's solubility parameters of the solvents used and the minimum statistical polymer unit for two different monomer molar ratio feeds (45%MAA−20% HEMA−35%EDMA, called P1, and 20%MAA−45% HEMA−35%EDMA, called P2) calculated by Hoftycer and van Krevelen.

Since the polymerization rates of the two or three monomers are similar, the composition of the copolymer could be defined by the initial molar monomers ratio feed.[33] The monomers used in this work have been chosen bearing in mind the conditions mentioned above,[24] and therefore, the minimum statistical polymer unit can be calculated by calculating the initial molar ratio between the monomers and cross-linker. We used 2.5% (w/v) of monomer mixture with respect to total volume (16 mL). This corresponds to a total number of moles of 0.003. Thus, the initial number of moles of each component is $n_{MAA} = 0.0014$, $n_{EDMA} = 0.0011$, and $n_{HEMA} = 0.0006$, and the molar ratios are as follows:

$$\frac{n_{MAA}}{n_{HEMA}} = 2.3, \quad \frac{n_{EDMA}}{n_{HEMA}} = 1.6, \quad \frac{n_{HEMA}}{n_{HEMA}} = 1$$

The minimum statistical polymer unit might be calculated by using the first multiple which provides three natural numbers for these molar ratios. In the case of P1, it is necessary to multiply the three molar ratios by 10 to get the lowest three natural numbers; thus the minimum statistical polymer unit is $(MAA)_{23}(HEMA)_{10}(EDMA)_{16}$. Using the same calculations, the minimum statistical polymer unit for P2 is formed by $(MAA)_4(HEMA)_9(EDMA)_7$.

4e. Characterization of the Different Polymeric Network Morphologies. Recently, we have developed a semiempirical model to determine the areas in which the polymeric network precipitate or are solvated. By using the model proposed by Medina-Castillo et al.,[24] we will determine the windows in which P1 and P2 either precipitate or are solvated in the ternary solvent mixture formed by toluene, 2-propanol, and acetonitrile. Figure 4 shows the windows of precipitation and solubilization of P1 and P2 polymeric systems. It shows two regions; one in which the polymeric growing chains are solvated during all the polymerization reaction ($\Delta G_{\text{mix}} < 0$) and thus it provides solvated copolymers; and the second one, in which the polymeric growing chains precipitate (when $\Delta G_{\text{prec}} < 0$) and provide several polymeric network morphologies. In this section, we will characterize, by $PD_{s,p,0}$

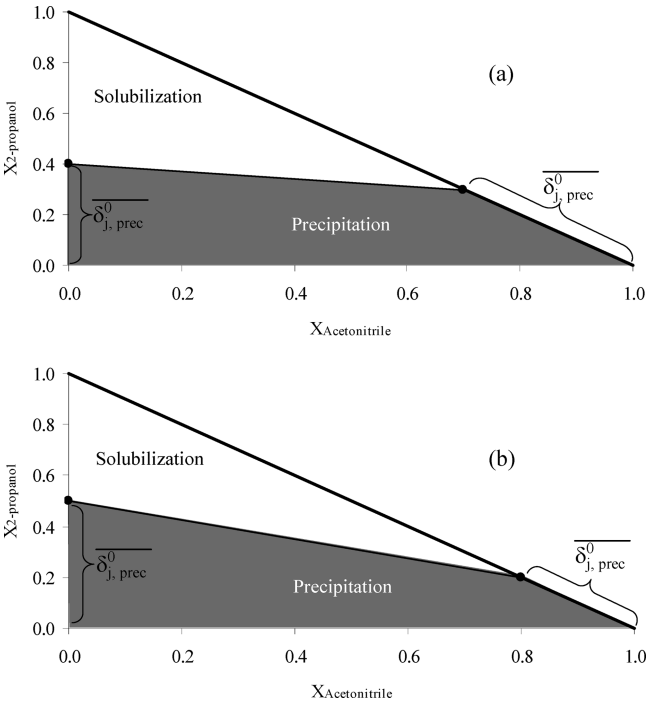

Figure 4. Regions of solubilization and precipitation of (a) system P1 and (b) system P2, obtained according to ref 24.

and $H_{s,p,0}$ values the different polymeric network morphologies found in this region.

The values of $PD_{s,p,0}$ and $H_{s,p,0}$ were calculated by eqs 11 and 12 (see Table 3), where Hansen's solubility parameters for the solvents were calculated by eqs 8 and the Hansen's solubility parameter of the polymer have been previously calculated in section 4d. (see Table 2).

Two experimental ellipsoids can be represented to distinguish between three regions: solvated copolymers, gel and spherical particles. These ellipsoids resulted from using:

$$\frac{PD_{s,p,0}}{a_i^2} + \frac{H_{s,p,0}}{b_i^2} = 1 \qquad (20)$$

where a_i and b_i for ellipsoid 1 are the maximum values of $PD_{s,p,0}$ and $H_{s,p,0}$ which provide solvated copolymers and for ellipsoid 2 are the maximum values of $PD_{s,p,0}$ and $H_{s,p,0}$ which provide gels (see Figure 5).

Figure 5 shows the three regions: the region formed by the copolymer solution, the region formed by gels, and the region formed by spherical particles. In addition, it is possible to see that nonspherical particles formed by homocoagulation processes result at very high values of $H_{s,p,0}$ and very low values of $PD_{s,p,0}$. This is because, under this conditions, small particles precipitated rapidly because they had high amount of hydroxyl groups and the solvent media could not solvate the early polymeric growing chains (the first minimum value of ΔG_{prec}; see Figure 2; high values of $H_{s,p,0}$ corresponds with low values of hydrogen bonding interactions). After precipitation, these small particles, due to their high amount of OH groups, interact with each other to reduce the number of OH groups exposed to the solvent and at the end the system is stabilized by non spherical particles formed by a homocoagulation process (second minimum value of ΔG_{prec}; see Figure 2) .

4f. Relationship between Flory's Parameter and the Particle Size of Spherical Particles. Table 3 also shows the values of the diameter, polydispersion index (PdI), particle area (considering the particles as spheres), initial Flory's parameter ($\chi_{s,p,0}$) and solubility parameter distance ($R_{s,p,0}$) for all the experiments performed. Diameter and PdI were calculated by dynamic light scattering, $R_{s,p,0}$ were calculated by eq 13 using the values of $PD_{s,p,0}$ and $H_{s,p,0}$ calculated in Section 4.d. and $\chi_{s,p,0}$ were calculated by using eq 9.

This shows that, for the P1 system, in the most of cases, solvated copolymers result when the Flory's parameter is lower than 2.4, whereas when the Flory's parameter is higher than 2.4, spherical particles are obtained. For the P2 system, solvated copolymer in most cases result when the Flory's parameter is lower than 3.5 whereas when the Flory's parameter is higher than 3.5, particles are spherical.

Figure 6 shows the relation between $\chi_{s,p,0}$ and particle area of the spherical particles. It shows that it is possible to establish a correlation between $\chi_{s,p,0}$ and the size of spherical particles; a decrease of $\chi_{s,p,0}$ increases of particle size and vice versa. Thus, expression 16 is corroborated.

Therefore, changing $\chi_{s,p,0}$ by changing the initial solvent compositions, we can control the particle size, over a wide range, without changing the monomer ratio feed.

4g. Relationship between $PD_{s,p,0}$ and $H_{s,p,0}$ with Particle Size of Spherical Particles. Figure 7 shows how $PD_{s,p,0}$ and $H_{s,p,0}$ change with the particle size. We find that smaller particles correspond to higher $PD_{s,p,0}$ values (lower dispersion and polar interactions between solvent and polymeric growing chains) and lower $H_{s,p,0}$ values (higher hydrogen bonding interactions between solvent and polymeric growing chains), and vice versa.

The polymeric growing chains of the polymeric systems under study (P1 and P2) have a high amount of hydroxyl groups. Thus, higher values of $H_{s,p,0}$ and lower values of $PD_{s,p,0}$ make early polymeric growing chains self-associated.[34] This boosts the average molecular weight at the I.C. point, and therefore an increase of the particle size obtained by precipitation.

On the other hand, lower values of $H_{s,p,0}$ and higher values of $PD_{s,p,0}$ avoid the self-association of early polymeric growing chains. As a result, the growth of early polymeric chains is due to monomer addition. Therefore, the average molecular weight at the I.C. point is lower than in the other case, and provides smaller particles.

In short, we can conclude that the average molecular weight of polymeric growing chains of P1 and P2 systems at the I.C. points, and therefore their particle size, can be controlled by the initial solvent composition.

4h. Encapsulation of Iron Oxide (Fe_3O_4) by Polymerization Precipitation. Polymerization precipitation can be used for successful encapsulation of Fe_3O_4 in different polymeric matrixes. In this work, we used polymerization precipitation to encapsulate Fe_3O_4 in the P1 and P2 hydrophilic polymer matrixes.

The encapsulation of Fe_3O_4 by precipitation polymerization has been undertaken in three steps: (1) conventional synthesis of hydrophobic magnetic nanoparticles using oleic acid (OA) (Fe_3O_4−OA); (2) encapsulation of Fe_3O_4−OA with an adequate cross-linked polymer matrix in order to change its polarity and allow the formation of stable dispersions in the precipitation media and, additionally, to provide adequate interactions between the polymeric matrix used to encapsulate the iron oxide and the polymeric growing chains during the polymerization precipitation; (3) encapsulation of the magnetic nanoparticles prepared in step 2 into hydrophilic polymer matrixes (P1 and P2) by polymerization precipitation.

Figure 8 shows the SEM and HREM images of these magnetic hybrid nanoparticles encapsulated by EDMA/MMA/HEMA (EDMA/MMA−Fe_3O_4−OA). They have a

Table 3. Size, Area, PdI, $H_{s,p,0}$, $PD_{s,p,0}$, $R_{s,p,0}$, Flory's Parameter, Yield, and Morphology of the Materials Prepared by Precipitation Polymerization of P1 and P2 Systems[a]

	size (nm)	area (m^2)	PdI	$H_{s,p,0}$ ($MPa^{1/2}$)	$PD_{s,p,0}$ ($MPa^{1/2}$)	$R_{s,p,0}$ ($MPa^{1/2}$)	$\chi_{s,p,0}$	% yield	morphology
system P1	n.d.	n.d.	n.d.	4.7	2.9	5.5	1.0	n.d.	SC
	n.d.	n.d.	n.d.	3.0	3.5	4.7	0.7	n.d.	SC
	n.d.	n.d.	n.d.	1.3	4.3	4.5	0.6	n.d.	SC
	n.d.	n.d.	n.d.	0.6	5.3	5.3	0.8	n.d.	SC
	n.d.	n.d.	n.d.	2.6	6.3	6.8	1.3	n.d.	SC
	n.d.	n.d.	n.d.	4.8	7.5	8.9	2.1	n.d.	SC
	n.d.	n.d.	n.d.	3.7	8.6	9.3	2.4	n.d.	SC
	n.d.	n.d.	n.d.	4.8	7.5	8.9	2.1	n.d.	SC
	n.d.	n.d.	n.d.	1.9	7.6	7.8	1.6	n.d.	SC
	n.d.	n.d.	n.d.	2.4	6.6	7.1	1.7	n.d.	SC
	n.d.	n.d.	n.d.	0.7	8.5	8.6	2.1	n.d.	SC
	n.d.	n.d.	n.d.	5.5	4.0	6.8	1.5	n.d.	SC
	n.d.	n.d.	n.d.	4.0	5.9	7.1	1.7	n.d.	SC
	n.d.	n.d.	n.d.	3.2	4.8	5.8	1.1	n.d.	SC
	n.d.	n.d.	n.d.	2.0	6.1	6.4	1.4	n.d.	SC
	n.d.	n.d.	n.d.	1.6	7.4	7.6	1.6	n.d.	SC
	n.d.	n.d.	n.d.	6.2	2.5	6.7	1.5	n.d.	G
	n.d.	n.d.	n.d.	7.6	2.4	8.0	2.2	n.d.	G
	n.d.	n.d.	n.d.	2.1	15.5	15.7	7.0	n.d.	G
	n.d.	n.d.	n.d.	6.7	5.7	8.8	2.5	n.d.	G
	311.6	3.0×10^{-13}	0.036	4.0	17.9	18.3	9.6	53	SP
	245	1.9×10^{-13}	0.004	4.9	19.0	19.6	11.1	53	SP
	900	2.5×10^{-12}	0.026	9.2	6.8	11.4	4.5	53	SP
	534	9.0×10^{-13}	0.036	7.9	10.3	13.0	5.4	50	SP
	265.7	2.2×10^{-13}	0.011	6.5	14.3	15.8	7.6	54	SP
	1471	6.8×10^{-12}	0.19	7.6	3.7	8.4	2.4	53	SP
	1072	3.6×10^{-12}	0.066	7.5	5.1	9.1	2.8	54	SP
	972.5	3.0×10^{-12}	0.18	7.5	6.8	10.1	3.4	53	SP
	662.6	1.4×10^{-12}	0.024	7.4	8.6	11.3	4.2	53	SP
	253	2.0×10^{-13}	0.012	4.4	18.4	19.0	10.3	53	SP
	440	6.1×10^{-13}	0.007	3.0	16.7	17.0	8.2	53	SP
	550	9.5×10^{-13}	0.08	2.6	16.1	16.3	7.6	53	SP
	650	1.3×10^{-12}	0.012	5.6	13.2	14.4	6.3	50	SP
	800	2.0×10^{-12}	0.026	6.7	8.6	10.9	3.8	52	SP
	1028	3.3×10^{-12}	0.05	8.1	5.2	9.6	3.1	53	SP
	600	1.1×10^{-12}	0.049	7.8	7.3	10.7	3.8	53	SP
	1250	4.9×10^{-12}	0.15	8.4	3.3	9.0	2.8	53	SP
	1300	5.3×10^{-12}	0.2	8.1	3.9	9.0	2.7	52	SP
	1320	5.5×10^{-12}	0.21	7.4	5.4	9.2	2.8	53	SP
	n.d.	n.d.	n.d.	10.3	2.8	10.6	4.1	n.d.	HC
	n.d.	n.d.	n.d.	11.5	3.2	11.9	5.3	n.d.	HC
	n.d.	n.d.	n.d.	10.4	4.1	11.2	4.5	n.d.	HC
system P2	n.d.	n.d.	n.d.	3.8	5.2	6.4	1.3	n.d.	SC
	n.d.	n.d.	n.d.	2.0	6.2	6.5	1.3	n.d.	SC
	n.d.	n.d.	n.d.	3.3	8.8	9.4	3.2	n.d.	SC
	n.d.	n.d.	n.d.	3.9	7.0	8.0	2.1	n.d.	SC
	n.d.	n.d.	n.d.	2.0	8.9	9.1	2.5	n.d.	SC
	n.d.	n.d.	n.d.	0.1	10.1	10.1	3.5	n.d.	SC
	n.d.	n.d.	n.d.	0.5	10.2	10.2	3.5	n.d.	SC
	n.d.	n.d.	n.d.	4.0	9.7	10.5	3.7	n.d.	SC
	n.d.	n.d.	n.d.	2.8	16.5	16.7	7.9	n.d.	G
	n.d.	n.d.	n.d.	5.4	4.3	6.9	1.6	n.d.	G
	500	7.9×10^{-13}	0.002	5.6	19.7	20.5	12.1	51	SP
	650	1.3×10^{-12}	0.009	4.7	18.6	19.2	10.6	53	SP
	1310	5.4×10^{-12}	0.094	9.7	1.8	9.9	3.5	53	SP
	1623	8.3×10^{-12}	0.038	8.4	2.6	8.8	2.2	53	SP
	1950	1.2×10^{-11}	0.110	6.9	3.4	7.7	2.1	54	SP
	1437	6.5×10^{-12}	0.170	9.1	3.3	9.7	3.3	52	SP
	1060	3.5×10^{-12}	0.010	9.2	4.6	10.3	3.6	52	SP
	1216	4.6×10^{-12}	0.100	10.4	2.6	10.7	4.1	56	SP
	1324	5.5×10^{-12}	0.08	9.2	6.0	11.0	4.1	53	SP
	1200	4.5×10^{-12}	0.06	7.8	6.8	10.4	3.5	53	SP
	850	2.3×10^{-12}	0.018	7.1	11.8	13.8	5.9	53	SP
	630	1.2×10^{-12}	0.018	6.4	15.6	16.8	8.5	54	SP
	508	8.1×10^{-13}	0.003	8.0	12.8	15.1	7.1	54	SP
	460	6.6×10^{-13}	0.018	6.4	17.3	18.4	10.1	52	SP
	650	1.3×10^{-12}	0.052	5.6	17.9	18.8	10.3	52	SP
	700	1.5×10^{-12}	0.005	8.3	11.7	14.4	6.6	53	SP
	1000	3.1×10^{-12}	0.003	9.3	7.5	11.9	5.2	55	SP
	n.d.	n.d.	n.d.	12.2	0.4	12.2	5.6	n.d.	HC
	n.d.	n.d.	n.d.	11.0	1.1	11.0	4.5	n.d.	HC
	n.d.	n.d.	n.d.	10.6	5.2	11.8	4.8	n.d.	HC

[a] Notes: n.d., nondetermined; SC, solvated co-polymers; G, gels; SP, spherical particles; HC, nonspherical particles formed by homocoagulation.

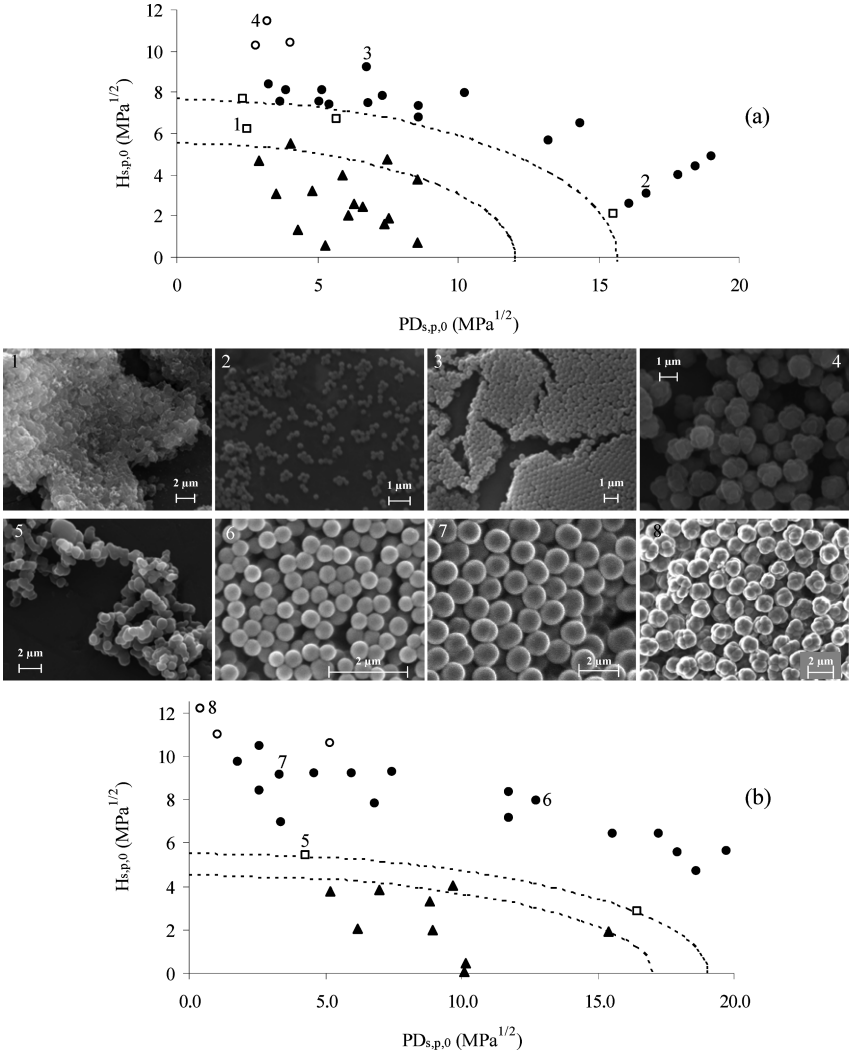

Figure 5. Regions of $H_{s,p,0}$ and $PD_{s,p,0}$ corresponding with the different polymeric network morphologies of (a) P1 and (b) P2 systems, and SEM pictures of these morphologies: 1 and 5 gels; 2, 3, 6, and 7 spherical particles; 4 and 8 nonspherical particles formed by homocoagulation.

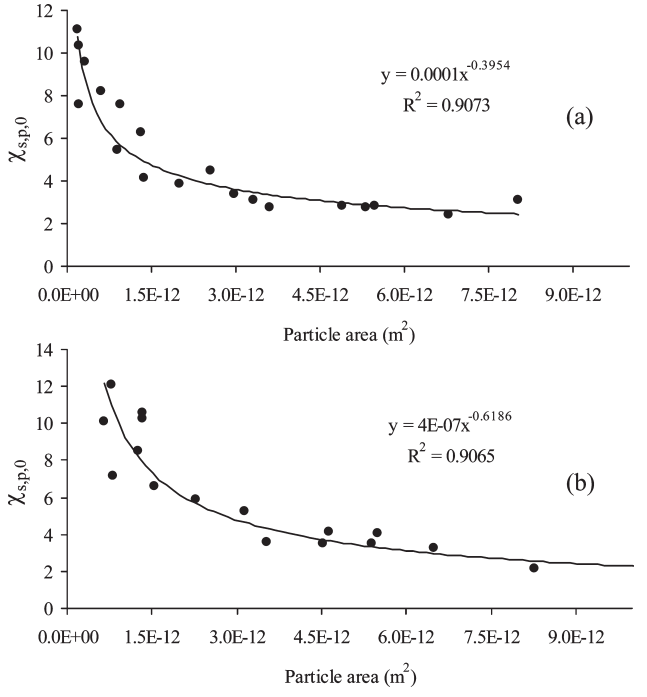

Figure 6. Relation between initial Flory's parameter and particle area for (a) P1 and (b) P2.

z-average of 100 nm with a polydispersion index (PDI) of 0.187 measured by DLS.

Figure 9 shows the SEM pictures of the particle resulting from polymerization in absence of Fe_3O_4−OA (1, 2, and 3) and HREM pictures of the particle resulting from polymerization in presence of Fe_3O_4−OA (1a, 2a, and 3a). It shows that, in all the cases, the magnetite is localized within of the polymeric matrix. This is because the magnetite was encapsulated has been made in a polymer matrix (EDMA/MMA/HEMA) which is thermodynamically compatible with the polymeric growing chains formed during polymerization; thus it avoids the phase separation.[31]

The magnetic particles 1a, 2a, and 3a are dispersed completely in water and are collected rapidly under a magnetic field (see Figure 10). We can also see in this figure how the magnetic particles are maintained dispersed and without decanting in water even after 25 min. After 25 min, the particles begin to decant.

In any case, further experiments need to be conducted in order to produce monodisperse nanoparticles of Fe_3O_4 encapsulated with an adequate polymer matrix and size control to be possible. Size control between 20 and 100 nm, could offer monodispersed perfectly defined core−shell particles using precipitation polymerization. In addition, how the size of the magnetic nanoparticles affect the final size of the core−shell particles should also be taken into account for future research.

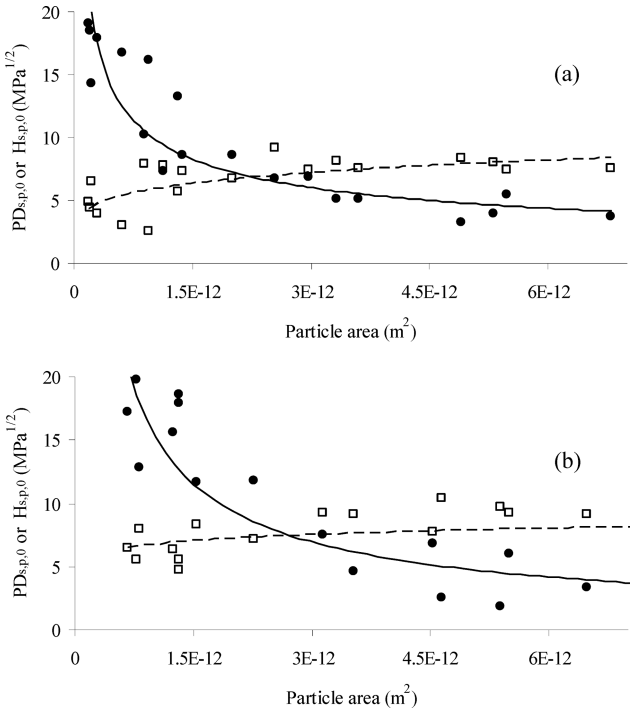

Figure 7. Relation between $PD_{s,p,0}$ (●, bold line), $H_{s,p,0}$ (□, dash line), and particle area for (a) P1 and (b) P2.

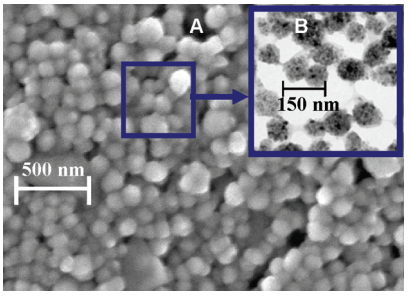

Figure 8. (A) SEM and (B) HRTEM pictures of EDMA/MMA/HEMA−Fe_3O_4−OA nanoparticles.

5. Conclusions

This work shows how to control the morphology and size of particles by controlling the solvent media in which precipitation polymerization is developed. The proposed model allows the preparation of different polymeric network morphologies (soluble copolymer, macrogels, gels, and spherical colloids) by controlling the different types of interactions (hydrogen-bonding forces, polar forces, and dispersion forces) between solvent and polymer. In addition, this model can be successfully used to correlate the particle size of spherical colloids with the Flory's parameter. Therefore, the model allows the control of the size in a wide range in order to synthesize spherical particles free of any stabilizers and without changing the monomer ratio feed.

The different polymeric network morphologies prepared in this work (spherical microparticles and gels) were used to introduce into magnetic properties. This work also shows the importance of thermodynamic compatibility between the polymeric growing chains and the matrix used to encapsulate the magnetite for adequate and homogeneous encapsulation of iron oxide within the matrix polymeric during the polymerization by precipitation. The results show that it is possible to control the size, chemical composition and the encapsulation of Fe_3O_4 within different hydrophilic polymeric matrixes by polymerization precipitation, enabling the design of magnetic particles free of any stabilizers. The particles designed in this ways can be extremely useful in many applications, for fundamental studies as well as

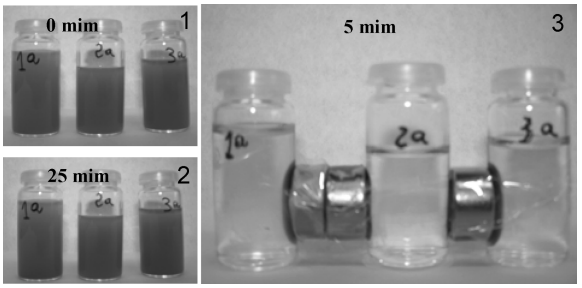

Figure 10. Magnetic particles (shown in Figure 9: 1a, 2a and 3a) dispersed in water. (1) Particles immediately after being dispersed in water. (2) Particles 25 min after being dispersed in water. (3) Particles completely collected under a magnetic field for 5 min.

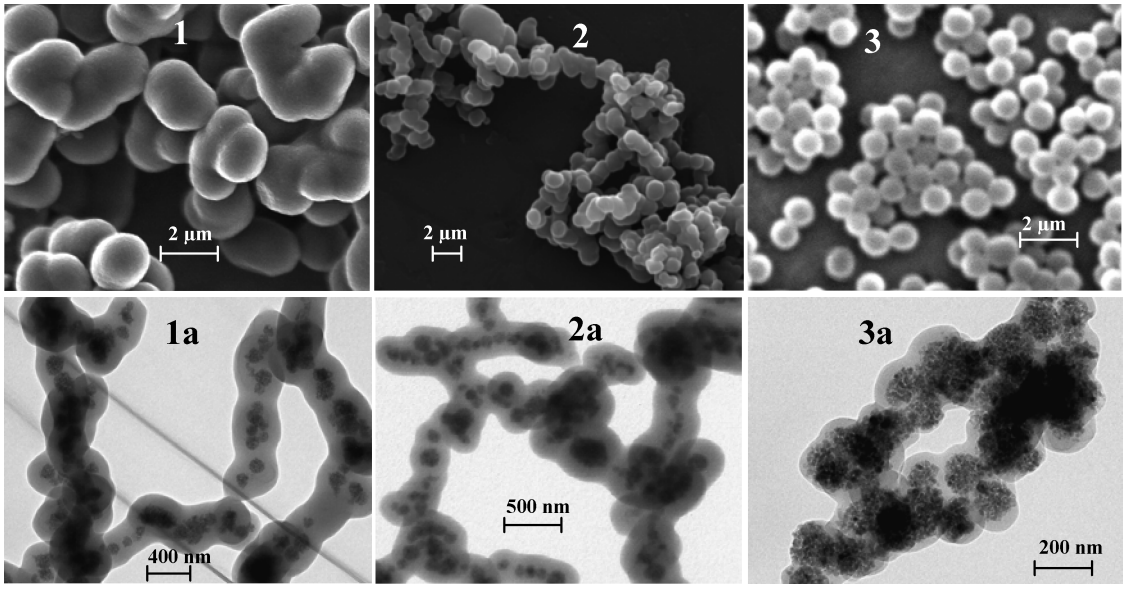

Figure 9. SEM pictures of precipitated particles which were synthetised in absence of Fe_3O_4 (1, 2, and 3) and HRTEM pictures of precipitated particles which were synthetised in the present of 5% of EDMA/MMA/HEMA-Fe_3O_4−OA nanoparticles (1a, 2a, and 3a).

industrial applications in fields such as drug delivery, nanopatterning, chemical and biosensing, and catalysis.

Acknowledgment. The authors express their thanks to the Spanish Ministry of Education (FPU grant reference AP2006-01144 and Project CTQ2008-01394) and the Regional Government of Andalusia (Excellence projects P07-FQM-02738 and P07-FQM-02625).

References and Notes

(1) Peng, X. G.; Schlamp, M. C.; Kadavanich, A. V.; Alivisatos, A. P. *J. Am. Chem. Soc.* **1997**, *119*, 7019–7029.
(2) Schirrer, R.; Lenke, R.; Boudouaz, J. *Polym. Eng. Sci.* **1997**, *37*, 1748–1760.
(3) Pathak, S.; Greci, M. T.; Kwong, R. C.; Mercado, K.; Prakash, G. K. S.; Olah, G. A.; Thompson, M. E. *Chem. Mater.* **2000**, *12*, 1985–1989.
(4) Okubo, M.; Nakagawa, T. *Colloid Polym. Sci.* **1994**, *272*, 530–535.
(5) McDonald, C. J.; Bouck, K. J.; Chaput, A. B.; Stevens, C. J. *Macromolecules* **2000**, *33*, 1593–1605.
(6) Mansky, P.; Liu, Y.; Huang, E.; Russell, T. P.; Hawker, C. J. *Science* **1997**, *275* (5305), 1458–1460.
(7) Halperin, A.; Tirrell, M.; Lodge, T. P. *Adv. Polym. Sci.* **1992**, *100*, 31–71.
(8) Fitch, R. M. *J.Elastomers Plastics* **1971**, *3* (3), 146–156.
(9) Li, W. H.; Stover, H. D. H. *J. Polym. Sci., Part A: Polym. Chem.* **1999**, *37*, 2899–2907.
(10) Goh, E. C. C.; Stover, H. D. H. *Macromolecules* **2002**, *35*, 9983–9989.
(11) Zhao, D.; Xinlin, Y.; Wenqiang, H. *Polym. Int.* **2007**, *56* (2), 224–230.
(12) Bai, F.; Huang, B.; Yang, X.; Huang, W. *Eur. Polym. J.* **2007**, *43*, 3923–3932.
(13) Shultz, A. R.; Flory, P. J. *J. Am. Chem. Soc.* **1952**, *74* (19), 4760–4767.
(14) Flory, P. J., *Principles of polymer chemistry*, 5th ed.; Cornell University Press: Ithaca, NY, 1992.
(15) Flory, P. J. *J. Am. Chem. Soc.* **1965**, *87*, 1833.
(16) Kurata, M., *Thermodynamics of polymer solution*; Harwood Academic Publishers: New York, 1982.
(17) Cheluget, E. L.; Weber, M. E.; Vera, J. H. *Chem. Eng. Sci.* **1993**, *48*, 1415–1426.
(18) Brandrup, J.; Immergut, E. H.; Grulke, E. A.; Abe, A.; Bloch, D. R., *Polymer handbook*, 4th ed.; Wiley Interscience: New Jersey, 1999.
(19) Hansen, C. M. *J. Paint Technol.* **1967**, *39*, 104.
(20) Barton, A. F. M. *Chem. Rev.* **1975**, *75*, 731–753.
(21) Lawson, D. D. *Appl. Energy* **1980**, *6*, 241–255.
(22) Hansen, C. M. *Hansen solubility parameters. A user's handbook*, 2nd ed.; CRC Press: Boca Raton, FL, 2007.
(23) Huang, J.-C.; Deanin, R. D. *Fluid Phase Equilib.* **2005**, *227* (1), 125–133.
(24) Medina-Castillo, A. L.; Fernandez-Sanchez, J. F.; Segura-Carretero, A.; Fernandez-Gutierrez, A. *Biosens. Bioelectron.* **2009**, *25*, 442–449.
(25) Froehling, P. E.; Koenhen, D. M.; Bantjes, A.; Smolders, C. A. *Polymer* **1976**, *17*, 835–836.
(26) Froehling, P. E.; Hillegers, L. T. *Polymer* **1981**, *22*, 261–262.
(27) Yanke, L.; Shufen, Z.; Jinzong, Y.; Qinghui, W. *Colloids Surf., A* **2004**, *248* (1−3), 127–133.
(28) Odian, G. *Principles of polymerization*, 4th ed.; Wiley Interscience: New Jersey, 2004.
(29) Elaissari, A. *Colloidal polymers. Synthesis and characterization* Marcel Dekker, Inc.: Lyon, France, 2003.
(30) Ashworth, A. J.; Price, G. J. *Macromolecules* **1986**, *19*, 358–361.
(31) Medina-Castillo, A. L.; Mistlberger, G.; Fernandez-Sanchez, J. F.; Segura-Carretero, A.; Klimant, I.; Fernandez-Gutierrez, A. *Macromolecules* **2010**, *43*, 55–61.
(32) Karger, B. L. *Anal. Chem.* **1978**, *50*, 2126–2136.
(33) Matyjaszewski, K.; Xia, J. *Chem. Rev.* **2001**, *101*, 2921–2990.
(34) Barton, A. F. M. *Pure Appl. Chem.* **1985**, *57*, 905–912.